International Journal of GEOMATE, May, 2016, Vol. 10, Issue 21, pp. 1854-1861
Geotec., Const. Mat. & Env., ISSN: 2186-2982(Print), 2186-2990(Online), Japan

QUANTIFICATION OF MACRODISPERSION IN LABORATORY-SCALE HETEROGENEOUS POROUS FORMATIONS

Kazuya INOUE [1], Tomoki KURASAWA [1] and Tsutomu TANAKA [1]

[1] Graduate School of Agricultural Science, Kobe University, Japan

ABSTRACT: Solute transport in groundwater is significantly influenced by the heterogeneity associated with spatial distribution of the hydraulic conductivity. Understanding solute transport behavior in heterogeneous flow fields is fundamental to develop appropriate models in aquifer management. In this study, laboratory-scale two-dimensional tracer experiments were carried out in a 1 m length, 1 m height and 0.03 m thickness sandbox to quantify solute macrodispersion phenomena in heterogeneous porous formation. Dye tracer of Brilliant Blue FCF mixed with NaCl was applied as a pulse type source and subsequent transport behavior of dye was recorded with digital camera. In addition to the spatial moment approach, temporal moment approach was also applied to estimate the longitudinal macrodispersivity by means of NaCl concentrations at an observation point in the flow field. The experimental results indicated that longitudinal and transverse macrodispersivity were larger than those in homogeneous formation. Moreover, it was revealed that both macrodispersivities in longitudinal and lateral directions have a non-dependency of the regional flow rates. Laboratory study was extended by the comparison with other studies, indicating adequate results in a suitable quantification range.

Keywords: Macrodispersion, Spatial moment, Temporal moment, Solute transport experiment, Heterogeneity

1. INTRODUCTION

The phenomenon of advective and dispersive mixing of solute in aquifers has been the subject of considerable research interest during the past few decades due to concerns on environmental impact and public health. In homogeneous porous media under laboratory conditions, the classical theory describing this spreading or dispersion of solute, based on Fickian process and flow, combines mass conservation and the time rate of change for the flux of a contaminant moving through a porous medium. On the other hand, geological media often possess very complex spatial patterns of hydraulic conductivity, leading to extremely complex solute transport behavior. That is, the Fick's law assumptions are no longer valid and the classical theory does not predict the amount of solute mixing. This phenomenon referred to as macrodispersion [12].

Understanding the characteristic behind such transport pathways related to macrodispersion is a crucial step to ensuring the reliable prediction of a contaminant behavior in a laboratory or a field. Field and laboratory scale experimental studies have been extensively conducted to examine macrodispersion in heterogeneous porous media under saturated or unsaturated flow conditions [11][12][14][15]. Several field experiments have also provided considerable insight into the transport process as affected by both small- and large-scale variations in the hydraulic properties [19]. The problem of field study is, however, that discrete point sampling provides only limited sampling spatially, and time required to collect samples limits sampling temporally. Such a difficulty to obtain detailed and comprehensive data sets directly in the field has led to the development of well-controlled laboratory experiments as useful tool to investigate macrodispersion process. In addition, image analysis techniques have become an attractive tool for a detailed monitoring of laboratory experiments at very high spatial and temporal resolution [18].

Macrodispersivities are often identified in the field by monitoring breakthrough curves at a limited number of observation wells [1]. However, in field tracer test, in general, breakthrough curves showing transitional concentration at a monitoring point cannot provide the transverse dispersivity. Contrary to the temporal moments, a snapshot of a cloud of solute particles in time expresses the dispersive variation in three directions in the aquifers, providing the estimates of spatial moments corresponding to the heterogeneity of concern [7].

The objectives of this study were to quantify the laboratory-scale longitudinal and transverse macrodispersivities using a non-invasive technique in conjunction with a dye tracer and to elucidate the solute transport behavior in two-dimensional heterogeneous porous formations under saturated conditions. Spatial and temporal moment approaches linked with image data of dye tracer behavior and variations of NaCl concentration, respectively, were utilized to rely on the difference

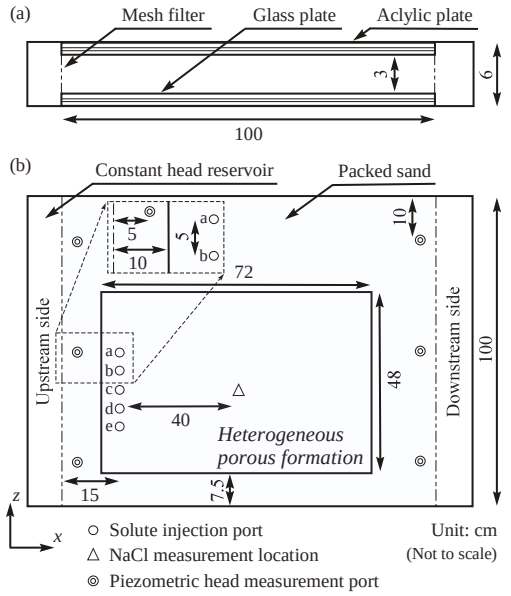

Fig. 1 Schematic diagram of laboratory-scale experimental apparatus: (a) Plane view and (b) vertical view.

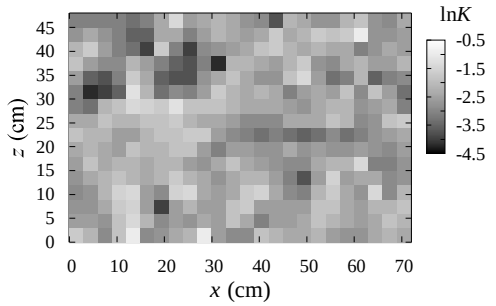

Fig. 2 Geostatistically generated porous formation with 0.307 of the heterogeneity.

between the two approaches.

2. LABORATORY-SCALE SOLUTE TRANSPORT EXPERIMENTS

2.1 Materials and Experimental Apparatus

Flow and transport observations are routinely made using dye tracers that allow visual qualitative, and in some cases quantitative, evaluations of plume evolution. Dyes are valuable tracers to clarify the movement of not only water but also solutes in porous media. For the purpose of visualization of solute transport phenomena, in this study, Brilliant Blue FCF, which is a synthetic color (color index 42090) having the hue of bright greenish blue and the nature of readily visible in soils, moderate mobile, and low toxicity [9][10],

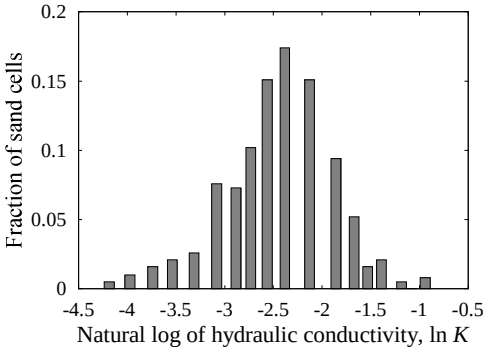

Fig. 3 The fraction distribution of the seventeen different materials.

was used as a dye tracer. NaCl was also mixed with dye tracer solution of Brilliant Blue FCF in order to observe the solute concentration of NaCl at a point in a flow field. The initial concentrations of Brilliant Blue FCF and NaCl were adjusted to 0.20 mg/cm^3 and 5.0 mg/cm^3, respectively. The initial concentration of dye tracer was determined to be low enough to avoid density-induced flow effects.

The intermediate-scale experiments were carried out in a two-dimensional horizontal laboratory tank (100 cm × 100 cm × 3 cm) packed with silica sand to create a heterogeneous medium with well-defined statistical properties. The flow tank was constructed from 1.5 cm acrylic and glass plates for the front and back respectively and stainless steel for the both sides and bottom. At the front side, the glass plate provided the opportunity of visual observation of migrating dye tracer, while 6 manometers established at the perforated acrylic plate were placed in the flow tank to determine piezometric heads. Constant head water reservoirs connected to the upstream and downstream ends of the tank were used to control the water flow. Schematic diagram of experimental apparatus is shown in Fig. 1.

The area referred to as the heterogeneous formation shown in Fig.1 was the primal area to create the heterogeneous porous formation using seventeen different sands reflecting heterogeneous field sites. The hydraulic conductivity distribution assumed to follow a log-normal probability density function [20][21] and was characterized by the geometric mean value of 0.0859 cm/s and the geometric variance of 0.307. Also it is assumed that the hydraulic conductivity distribution exhibits spatially-correlated structure defined by an exponential covariance function with correlation scale of 6 cm. Block kriging [6][13] was used to geostatistically generate the heterogeneous porous formation based on the fraction distribution of the seventeen different materials. Hydraulic

Table 1 Experimental cases.

Case	Injection port	Flow rate (cm^3/min)
Homogeneous cases		
	1 point (c)	297
	3 points (c,d,e)	297
	5 points (a,b,c,d,e)	297
Heterogeneous cases		
	1 point (c)	297
	3 points (c,d,e)	297
	5 points	101
	5 points	184
	5 points	297

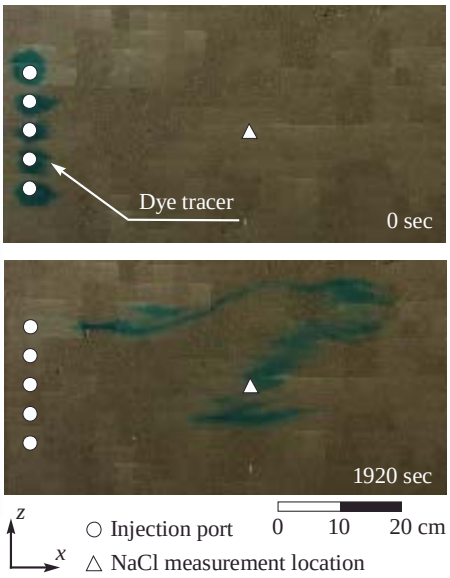

Fig. 4 Representative images of dye tracer transport in heterogeneous formation.

conductivity distribution employed in this study and the fraction distribution of soils are shown in Fig. 2 and Fig. 3, respectively. Addition to the heterogeneous porous formation, as the base case of solute transport in homogeneous porous media, soil material having the logarithm hydraulic conductivity of -2.13 comprised a homogeneous porous formation.

2.2 Experimental Procedure

Packing of the materials with 24 and 16 cells in the *x* and *z* directions, respectively, was carried out under saturated conditions in order to avoid air entrapment. Each sand cell had 3 cm and 3 cm in both directions. The prescribed packing structures were established to transparent sheets described all sand cell locations and attached to the glass plate of flow tank. As the first step before creating heterogeneous porous packing, as shown in Fig 1, the soil material with -1.18 of the geometric mean of the hydraulic conductivity was filled in 7.5 cm layer at the bottom of the tank through the process of compaction. In heterogeneous packing, the materials comprising each cell were packed in 3 cm layers using narrow dividers with the thickness of 1 cm to establish sharp connectivity between cells. The dividers were removed as packing progressed. The rest of upper area was filled by the same soil material ($\ln K = -1.18$) in the same manner in 6 cm layers.

After packing, water was applied to the flow tank under a specific hydraulic gradient controlled by constant head water reservoirs at the upstream and downstream sides, while maintaining saturated condition of porous media. A steady saturated flow field was established in the flow tank when fluctuations in the observed drainage rate, which was effluent from the constant head water reservoir at the downstream side and piezometer reading at water pressure measurement points became negligible. In tracer experiments, to examine the effect of variation of flow rate on macrodispersion phenomena, solute transport experiments were carried out for flow rates of 101, 184 and 297 cm^3/min.

After steady flow field was established, dye tracer of Brilliant Blue FCF mixed with NaCl was released from one injection port of c, three injection ports of b, c and d or five injection ports from a to e whose locations are depicted in Fig.1. Experimental cases are listed in Table 1. The solution with 25 cm^3 in each injection port was injected for 30 seconds. During the experiment, the profiles of solute migration were recorded using a digital camera approximately 100 cm located away from the water flow tank.

3. ESTIMATION OF SOLUTE MACRODISPERSION USING MOMENT APPROACHES

3.1 Transport Process and Image Calibration

As an example of solute migration, the typical image obtained during the tracer experiments is shown in Fig.4. Each of the pixels representing an image has a pixel intensity which describes how bright that pixel is. Data recorded by the digital camera successfully indicated different pixel intensities in dye tracer distributions, suggesting

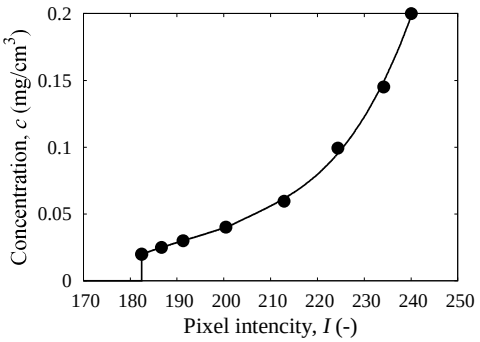

Fig. 5 Example of relation between the pixel intensity and the dye tracer concentration.

different concentrations of the dye tracer. In order to establish a relationship between the color intensity and dye concentration, calibrations were performed and analyzed with solutes of known concentrations of dye. Example of regression curve to calculate dye concentrations is shown in Fig. 5.

3.2 Spatial Moment Approach

Spatial moments of aqueous concentrations distributed in space are calculated based on the spatial moment approach [20]. Spatial moments are calculated from digital image at given times as follows:

$$M_{ij}(t) = \int_{-\infty}^{\infty}\int_{-\infty}^{\infty} c(x,z,t)x^i z^j dxdz \tag{1}$$

where x and z are the Cartesian coordinates, c is the solute concentration, t is the time, M_{ij} is the spatial moments associated with the distribution of tracer plume at a certain time, and i and j are the spatial order in the x and z coordinates, respectively. Based on the regression curves relevant to the dye concentration and pixel intensity described avobe, the pixel intensity distribution can be converted to a concentration distribution by the calibration, providing an analogy between Eq.(1) and Eq.(2) [17]

$$M_{ij}(t) = \int_{-\infty}^{\infty}\int_{-\infty}^{\infty} H(x,z)I(x,z,t)x^i z^j dxdz \tag{2}$$

where $H(x,z)$ is the area per unit pixel and $I(x,z,t)$ is the intensity at a corresponding pixel.

The centroid of concentration distribution of dye is able to be calculated as the normalized first-order spatial moment.

$$x_c = \frac{M_{10}}{M_{00}}, \quad z_c = \frac{M_{01}}{M_{00}} \tag{3}$$

where x_c and z_c are the centroid locations of plume concentration distribution in the x and z coordinates, respectively. The second order spatial moments are also computed as follows.

$$\sigma_{ij} = \begin{pmatrix} \frac{M_{20}}{M_{00}} - x_c^2 & \frac{M_{11}}{M_{00}} - x_c z_c \\ \frac{M_{11}}{M_{00}} - z_c x_c & \frac{M_{02}}{M_{00}} - z_c^2 \end{pmatrix} \tag{4}$$

where σ_{ij} is the second order spatial moments. Longitudinal and transverse macrodispersivities from spatial moments of the distributed tracer plume are calculated as [17][20]

$$A_L = \frac{1}{2}\frac{\sigma_{xx}}{\xi_c}, \quad A_T = \frac{1}{2}\frac{\sigma_{zz}}{\xi_c} \tag{5}$$

where A_L is the longitudinal macrodispersivity, A_T is the transverse macrodispersivity and ξ_c is the travel distance of the center of tracer plume in the mean flow direction at a given time t.

3.3 Temporal Moment Approach

The temporal moment approach was used to characterize the breakthrough data at NaCl measurement location. The jth normalized absolute temporal moments, $\mu_j(x)$, and the jth central temporal moments around the mean, $\mu'_j(x)$, are very useful descriptors of breakthrough curves (BTCs). The first-order temporal moment corresponds to the mean arrival time of solute, while the second-order temporal moment is an analogy with the statistical dispersion [8]

$$\mu_j(x,z) = \frac{\int_0^{\infty} t^j c_m(x,z,t)dt}{\int_0^{\infty} c_m(x,z,t)dt} \tag{6}$$

$$\mu_j(x,z) = \frac{\int_0^{\infty} (t-\mu_1)^j c_m(x,z,t)dt}{\int_0^{\infty} c_m(x,z,t)dt} \tag{7}$$

where $c_m(x,z,t)$ represents the time variation of the NaCl concentrations at the monitoring locations, and j is the nonnegative integer corresponding to the order of concern. Longitudinal macrodispersivities using temporal moments are calculated as

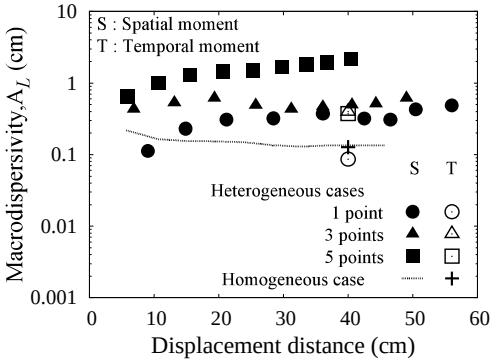

Fig. 6 Longitudinal macrodispersivity variation identified with spatial and temporal moments in heterogeneous and homogeneous formation.

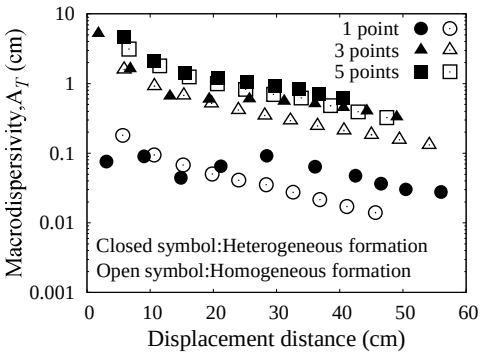

Fig. 7 Transverse macrodispersivity variation identified with spatial moments in heterogeneous and homogeneous formation.

$$A_L(\zeta_p) = \frac{\zeta_p}{2} \frac{\mu_2'(\zeta_p)}{(\mu_1(\zeta_p))^2} \tag{8}$$

where ζ_p is the distance from the source of solute injection to the observation point. Ideally, as for temporal moment approach, several observation points along a line comprise one cross-sectional plane to capture all dye concentrations passing through this plane, which is referred to as the control plane. However, to reflect a field situation where a quite limited number of observation points may exist, Eq.(8) is applied to a single observation point in this study.

4. RESULTS AND DISCUSSION

4.1 Longitudinal Macrodispersivity

Longitudinal macrodispersivity values obtained from spatial and temporal moments in heterogeneous and homogeneous formations are shown in Fig. 6 as a function of the mean displacement distance of dye tracer distribution. Longitudinal macrodispersivity estimates in homogeneous formation remain constant during the course of solute transport whereas longitudinal macrodispersivity estimates in heterogeneous formation exhibit the increase tendency with the increase of displacement distance. This is attributed to the distribution of hydraulic conductivity comprising flow fields and exhibits the evidence occurring macrodispersion phenomena in heterogeneous porous formation. Hence, these results demonstrate that the scale effect of macrodispersion can be observed under controlled laboratory conditions. In heterogeneous formation, longitudinal macrodispersivity values obtained from spatial moments show a dependency on the number of injection ports, or on the initial plume length in the *z* direction. This is due to the difference of the inherent heterogeneity associated with the solute transport pathway, indicating that local heterogeneity in porous formation affects the degree of solute dispersion.

In homogeneous formation, longitudinal macrodispersivity estimates using temporal moments are almost identical to the macrodispersivity estimates obtained from spatial moments. This may suggest that single monitoring point leads to a plausible result in homogeneous porous formations if a direction from a solute injection port to a monitoring point is parallel to the regional flow direction. Contrary to this, in heterogeneous formation except for the case with three injection points, a marked difference between longitudinal macrodispersivity estimates from spatial and temporal moments appears. This indicates that single monitoring location is insufficient to capture the primal characteristics of solute transport as breakthrough curves and to identify a reliable estimate. As aforementioned above, temporal moment approach is inherently applied in the cross-sectional plane using many observation points but a single observation point. Hence, it is revealed that a single observation point can be applied to the estimation in homogeneous porous media.

4.2 Transverse Macrodispersivity

The results of transverse macrodispersivity estimates obtained from spatial moments are shown in Fig. 7 as a function of the displacement distance of solute. The difference of estimates between homogeneous and heterogeneous porous formations appears in transverse macrodispersivity variation shown in Fig.7, especially in larger displacement distance. This is because the shapes

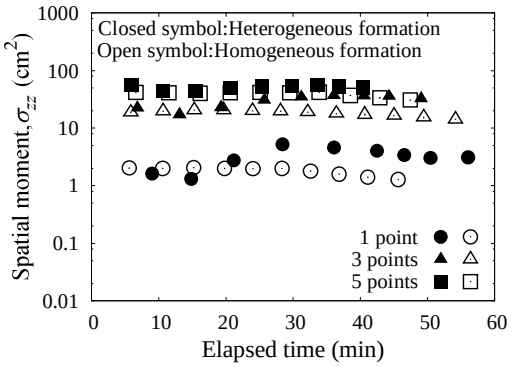

Fig. 8 Variation of spatial moment of σ_{zz} in each formation

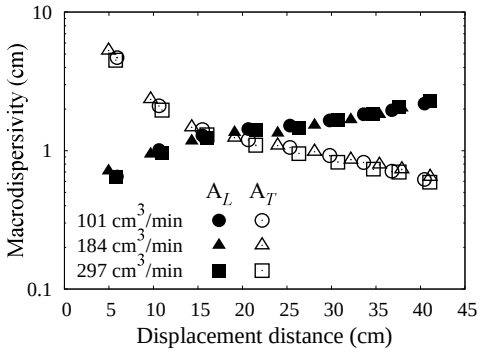

Fig. 9 Macrodispersivity estimates obtained from spatial moments under various flow rate conditions.

of tracer plumes become complex and irregular according to the preferential pathlines of solute in heterogeneous formation, leading to the transverse macrodispersivity estimates in heterogeneous formation relative to those in homogeneous formation.

The values of the transverse macrodispersivity indicate a dependency on the number of injection ports in the *z* direction and show the decrease tendency. To clarify this variation, the results of the second spatial moments in the *z* direction σ_{zz} as a function of elapsed time are shown in Fig. 8. The results of σ_{zz} variation exhibit a dependency on the corresponding plume scale in the *z* direction. The geometrical elongation of the initial tracer distribution in the *z* direction provides a higher value of σ_{zz}. In this experiment, the velocity component in the *z* direction is relatively small to that in the *x* direction. Therefore, as shown in Fig.8, the results of σ_{zz} remain constant during the solute transport, resulting in larger values of the transverse dispersivity associated with the source length in the *z* direction. This feature leads to a decrease tendency of the transverse macrodispersivity, which is computed by the ratio of the second order spatial moment to the first order spatial moment expressed in Eq.(5). Although multiple-source injection may lead to larger transverse macrodispersivity estimates, it seemed that variation of transverse macrodispersivity associated with the heterogeneity is more pronounced with decreasing source size in the *z* direction.

4.3 Effect of Flow Rate

In order to examine the effect of variation of flow rate on macrodispersion phenomena, three experimental cases with the initial dye release from five injection ports were performed at various flow rates of 101, 184 and 297 cm^3/min. Figure 9 shows macrodispersivity estimates obtained from spatial moments at three flow rates. Longitudinal and transverse macrodispersivities have a non-dependency of flow rate. This tendency agrees with earlier work [22], suggesting the reliability of estimates under the flow rate condition employed in this study.

4.4 Comparison with other studies

Several factors including the porosity, the heterogeneity, the travel distance and the correlation length of hydraulic conductivity affect the degree of macrodispersion in porous media [8][12]. Table 2 compares the longitudinal and transverse macrodispersivities obtained in this study with a few results reported in the literature, which were conducted in similar situations. Estimate range for both macrodispersivities is in good agreement with other studies, ensuring the validity of obtained results in this study. Especially, the obtained results are similar to the results of McNeil et al. [18] where cell blocks of sand were utilized to comprise the heterogeneous porous formation. The evolution nature of the longitudinal and transverse macrodispersivities may be utilized for many purposes including contaminant transport modeling in a field as well as in a laboratory, water supply issues using a pumping well, thus leading to the resource protection.

5. CONCLUSION

In this study, the behavior of macrodispersion in heterogeneous and homogeneous formations was assessed through intermediate-scale solute transport experiments. Longitudinal and transverse macrodispersivities were identified using spatial

Table 2 Comparison of estimates in longitudinal and transverse macrodispersivities.

Longitudinal macrodispersivity (cm)	Transverse macrodispersivity (cm)	Mean travel distance (cm)	Reference
0.487– 2.07	0.0278	40– 56	This study (spatial moments)
0.0864– 0.373	n.d.	40	This study (temporal moments)
0.62 – 7.1	0.030 – 0.87	28 – 60	Inoue et al. [15]
0.41 – 1.2	0.35 – 0.73	45 – 56	Inoue et al. [16]
1.7 – 6.0	n.d.	33	Aggelopoulos and Tsakiroglou [2]
0.20 – 10.0	n.d.	50 – 70	Chao et al. [4]
2.3 – 5.9	n.d.	40 – 80	Danquigny et al. [5]
2.76	n.d.	100	Huang et al. [14]
n.d.	0.010	n.d.	Beaudoin and de Dreuzy [3]
4.6	0.019	120 – 160	McNeil et al. [18]

and temporal moment approaches using the dye tracer distribution and NaCl concentration, respectively. The following findings have been clarified.

1. Longitudinal and transverse macrodispersivity estimates obtained from spatial moments based on the distributions of dye tracer plume in heterogeneous formation were larger than those in homogeneous formation.
2. Longitudinal and transverse macrodispersivity values obtained from spatial moments in heterogeneous formation show a dependency on the plume-scale in the *z* direction.
3. In homogeneous formation, longitudinal macrodispersivity estimates using temporal moments are almost identical to the macrodispersivity estimates obtained from spatial moments. On the other hand, in heterogeneous formation, a marked difference between longitudinal macrodispersivity estimates from spatial and temporal moments appeared.
4. Under the flow rate conditions adopted in this study, the values of longitudinal and transverse macrodispersivities showed a non-dependency to the regional flow rates employed in this study.

6. REFERENCES

[1] Adams EE, Gelhar LW, "Field study of dispersion in a heterogeneous aquifer 2. spatial moments analysis", Water Resour. Res. 28(12), 1992, pp.3293-3307.

[2] Aggelopoulos CA, Tsakiroglou CD, "Quantifying soil heterogeneity from solute dispersion experiments", Geoderma, 146, 2008, pp.412-424.

[3] Beaudoin A, de Dreuzy J-R, "Numerical assessment of 3-D macrodispersion in heterogeneous porous media", Water Resour. Res., 49, 2013, pp.2489-2496.

[4] Chao HC, Rajaram H, Illangasekare TH, "Intermediate-scale experiments and numerical simulations of transport under radial flow in a two-dimensional heterogeneous porous medium", Water Resour. Res., 36(10), 2000, pp.2869-2884.

[5] Danquigny C, Ackerer P, Carlier JP, Laboratory tracer tests on three-dimensional reconstructed heterogeneous porous media", J. Hydrol., 294, 2004, pp.196-212.

[6] Deutsch CV, Journel AG, "GSLIB: Geostatistical software library and user's guide", Oxford University Press, 1992, 340p.

[7] Fadili A, Ababou R, Lenormand R, "Dispersive particle transport: identification of macroscale behavior in heterogeneous stratified subsurface flows", Math. Geol., 31(7), 1999, pp.793-840.

[8] Fernàndez-Garcia D, Illangasekare TH, Rajaram H, "Difference in the scale-dependence of dispersivity estimated from temporal and spatial moments in chemically and physically heterogeneous porous media", Water Resour. Res., 28, 2005, pp.745-759.
[9] Flury M and Flühler H, "Tracer characteristics of brilliant blue FCF", Soil Sci. Soc. Am. J., 59, 1995, pp.22-27.
[10] Forrer I, Kasteel R, Flury M, Flühler H, "Longitudinal and lateral dispersion in an unsaturated field soil", Water Resour. Res., 35(10), 1999, pp.3049-3060.
[11] Forrer I, Papritz A, Kasteel R., Flühler H., Luca D. "Quantifying dye tracers in soil rofiles by image processing", Euro. J. Soil Sci., 51, 2000, pp.313-322.
[12] Gelhar LW, Welty C, Rehfeldt KW, "A critical review of data on field-scale dispersion in aquifers", Water Resour. Res., 28(7), 1992, pp.1955-74.
[13] Ghori SG, Heller JP, Singh AK, "An efficient method of generating random permeability fields by the source point method", Math. Geol., 25(5), 1993, pp.559-572.
[14] Huang K, Toride N, van Genuchen MTh, "Experimental investigation of solute transport in large, homogeneous, and heterogeneous, saturated soil columns", Transp. Porous Media, 18, 1995, pp.283-302.
[15] Inoue K, Fujiwara T, Kurasawa T, Tanaka T, "Quantification of solute macrodispersion phenomena and local heterogeneity using intermediate-scale solute transport experiments in heterogeneous porous formations", J. JSCE A(2), 70(2), 2015, (in Japanese) (in press).
[16] Inoue K, Fujiwara T, Tanaka T, " Intermediate-scale solute transport experiments for identifying solute dispersion parameters in heterogeneous porous media using spatial and temporal moment approaches", J. JSCE A(2), 69(2), 2013, pp.I_9-I_18(in Japanese) .
[17] Inoue K, Kobayashi A, Suzuki K, Takenouti R, Tanaka T, "A new approach for estimating macrodispersivity using dye tracer and spatial moment analysis", Annual J. Hydraulic Eng., JSCE, 55, 2011, pp.613-618 (in Japanese).
[18] McNeil JD, Oldenborger GA, Schincariol RA, "Quantitative imaging of contaminant distributions in heterogeneous porous media laboratory experiments", J. Contam. Hydrol., 84, 2006, pp36-54.
[19] Sudicky EA, "A natural gradient experiment on solute transport in a sand aquifer: Spatial variability of hydraulic conductivity and its role in the dispersion process", Water Resour. Res., 22(13), 1986, pp.2069-82.
[20] Tompson AFB, Gelhar LW, "Numerical simulation of solute transport in three-dimensional, randomly, heterogeneous porous media", Water Resour. Res., 26(10), 1990, pp.2541-62.
[21] Turcke MA, Kueper BH, "Geostatistical analysis of the Borden aquifer hydraulic conductivity field", J. Hydrol., 178(4), 1996, pp.223-240.
[22] Zinn B, Meigs LC, Harvey CF, Haggerty R, Peplinski WJ, Von Schwerin CF, "Experimental visualization of solute transport and mass transfer process in two-dimensional conductivity fields with connected region of high conductivity", Environ. Sci. Technol, 38, 2004,pp.3916-3926.

International Journal of GEOMATE, May, 2016, Vol. 10, Issue 21, pp. 1854-1861
MS No. 5163 received on June 15, 2015 and reviewed under GEOMATE publication policies.

Corresponding Author: Kazuya INOUE